



Lawrence Livermore National Laboratory

LLYMP9502082
February 15, 1995

WBS: 1.2.9

L. Dale Foust
Technical Project Officer
CRWMS-M&O
101 Convention Center Drive, M/S 423
Las Vegas, NV 89109

**Subject: Lawrence Livermore National Laboratory (LLNL) Monthly Status Report
(SCPB:N/A)**

Dear Dale:

I am pleased to submit the LLNL monthly report under our status as a CRWMS-M&O teammate.

The report has much the same format as previous reports to the Yucca Mountain Site Characterization Office (YMSCO), except that financial information required in Participant Monthly Reports has not been included. LLNL financial data were reported directly to YMSCO again this month because we have not yet transitioned into the M&O accounting system.

If you require further information, please contact James Blink at (702) 794-7157.

Sincerely yours,


for Willis L. Clarke
LLNL-CRWMS Manager

WLC/JAB/cjp

Enclosure

cc/enc: See Attached Distribution List
LLNL-CRWMS LRC



Recycled

LAWRENCE LIVERMORE NATIONAL LABORATORY
(LLNL)
YUCCA MOUNTAIN SITE CHARACTERIZATION PROJECT
(YMP)
STATUS REPORT

January 1995

EXECUTIVE SUMMARY

1) **WBS 1.2.2.4.1, Spent Fuel:** Unsaturated dissolution drip tests of spent fuel are being conducted at Argonne National Laboratory under Lawrence Livermore Laboratory sponsorship. The cesium gamma results for the leachate and vessel strip solutions (after 750 days of reaction) were compared to determine if the cesium remained in the leachate. The percentage of cesium sorbed on the test vessels differs as a function of drip rate. For low drip rate tests, 99% of the cesium was sorbed on the stainless vessel walls; whereas for high drip rate tests, 99% of the cesium was in the leachate. Since the leachate of the four tests have comparable pHs (6.8-7.2), other factors appear to be responsible for this behavior.

2) **WBS 1.2.2.4.1, High Level Waste:** The N3 unsaturated dissolution tests, performed on actinide-doped West Valley ATM-10 glass, being conducted at Argonne National Laboratory under Lawrence Livermore National Laboratory sponsorship were sampled on 1/12/95. They have been ongoing for 90 months. Sequential filtering was performed, and colloidal samples for analytical electron microscopy analysis were taken from three tests. An apparent variation among the test samples regarding the corrosion of the stainless steel components is emerging. Thus, interactions between waste package components could be important conduits for reaction and potential methods to mobilize radionuclides.

3) **WBS 1.2.2.5.1, Metallic Barriers:** The computational investigation at LLNL of how permanent pit growth cessation affects the damage function (i.e., the distribution of pit depths) continued. In general, the effect of pit growth cessation is the ultimate development of a static distribution with essentially an exponential-like decay in the number of pits as a function of depth. As the halt probability decreases, the rate of this decay decreases and the distribution broadens. Experimental data suggest that the pit depth distribution following long exposure times is more complex than this; typically, it contains a significant intermediate peak. Of course, it is necessary to explore a wider combination of growth and cessation values to confirm the generality of these observations. The major goal is to determine if distributions similar to those observed experimentally can be simulated using this approach.

4) **1.2.2.5.1, Metallic Barriers:** Experiments at Argonne National Laboratory under Lawrence Livermore National Laboratory sponsorship are measuring the stress corrosion cracking (SCC) susceptibility of candidate waste container materials under a variety of environmental, metallurgical, and mechanical stress conditions relevant to a repository. Research activities deal with fracture mechanics crack-growth-rate determinations on Incoloy 825, Titanium Grade 12, Hastelloy C-4, and Hastelloy C-22. Crack growth rate tests using standard compact tension fracture mechanics specimens were conducted on Incoloy 825 in an earlier phase of the program. Additional tests were initiated on Ti Grade 12, Hastelloy C-4, Hastelloy C-22, and on a new heat of Incoloy 825 in FY94. Preliminary data show that the crack propagates faster in the Titanium

Grade 12 specimen than in the Hastelloy specimens by an order of magnitude, in J-13 well water with a specific (accelerated) loading condition.

5) **WBS 1.2.3.1, Site Investigations Coordination and Planning (Groundwater Travel Time Distribution and Repository Performance):** Bounding calculations at LLNL (which assume an Engineered Barrier System that minimally meets the subsystem requirements of substantially complete containment and controlled release) suggest that, *in a strongly heterogeneous system with a large mean travel time*, a rather large fraction (up to 30%) of the total groundwater flux could have a travel time much less than 1,000 years and still allow satisfactory containment of radionuclides within the geologic control volume. In addition, the system must be somewhat heterogeneous to simultaneously account for the observed frequency of occurrence of bomb-pulse material at depth and to demonstrate total system compliance.

6) **WBS 1.2.3.12.3, Mechanical Attributes of the Waste Package Environment:** A second suite of uniaxial compression tests was conducted at LLNL on a sample block of Topopah Spring Tuff that measures 64 x 33 x 25 cm in size. Noticeable spalling occurred at several locations on the block. This was not observed during the first cycle of testing and indicates that subcritical crack growth occurs even at very low stresses in this rock when it is subject to cyclic loading. This may be relevant for evaluating the effect of seismic shaking of a repository over long times and at elevated temperature and humidity.

DELIVERABLES

LLNL Deliverables Met

(January 1995)

Milestone	WBS 1.2.	Planned Date	Completion Date	Description
MOL215	2.5.1	12-31-94	01-03-95	Update Scientific Investigation Plan
MOL180	2.5.1	01-31-95	01-31-95	Degradation Mode Survey of TI-Base Alloys
MOL78	3.10.1	10-31-94	01-26-95	Report on Code Model Capability Guidelines
MOL61	3.10.2	01-30-95	01-30-95	Study Plan - Characterization Techniques of AZ
MOL62	3.10.2	11-30-94	01-17-95	Data report on Small Block Tests to YMSCO
MOL25	3.12.1	12-31-94	01-20-95	Review of Existing Coupled Code Capabilities
MOL159	3.12.3	01-13-95	01-13-95	MOL203 Status (Geomechanical Measurements)
MOL130	3.12.5	02-03-95	01-31-95	MOL129 Status (Continuous Swipe Tests in the ESF #1)
MOL157	9.2.2	01-31-95	01-31-95	Internal Procedures to Reflect PACS Operations
MOL270	11.1	01-16-95	01-09-95	Quarterly Report #1

LLNL Deliverables Not Met

(January 1995)

Milestone	WBS 1.2.	Planned Date	Projected Date	Description	Comment
NOL32	3.12.2	01-31-95	02-28-95	Submit Study Plan (Modeling)	note 1

Note 1: This projected date was agreed upon by A. Simmons, YMSCO Team Leader, on 1-11-95. A
C/SCR is in preparation.

LLNL Deliverables Scheduled for the Next Reporting Period

(February 1995)

Milestone	WBS 1.2.	Planned Date	Description	Comment
MOL119	3.12.2	02-28-95	Resolve Study Plan (Lab) Comments	
MOL156	3.12.3	02-10-95	MOL204 Status (3D Discrete Element Computer Code)	
MOL248	3.12.4	02-17-95	NDE on a Sector from each Mfr. of Frame Sectors	note 2

Note 2: A C/SCR is in preparation to delete this milestone.

ISSUES AND CONCERNS

None that were not previously reported.

TECHNICAL SUMMARY

1.2.1. SYSTEMS ENGINEERING

1.2.1.5 Special Studies

Modeling Support for the Thermal Loading Systems Study

Investigation continued of various alternative thermal loading designs for the localized disturbance concept with emphasis on identifying the upper range of areal mass loading.

1.2.2. WASTE PACKAGE

1.2.2.1 Waste Package Coordination and Planning

1.2.2.4 Waste Form

1.2.2.4.1 Spent Fuel

Spent Fuel Oxidation

Building 325 at Pacific Northwest Laboratory (PNL) will reopen the week of February 3rd. Final revisions have been completed on the activity plan for the Thermogravimetric Apparatus (TGA) work.

Spent Fuel Dissolution

D-20-43, Unsaturated Dissolution Tests with Spent Fuel

Spent fuel is being tested under unsaturated conditions at 90°C to evaluate its long-term performance in the potential repository at Yucca Mountain. The tests monitor the leach/dissolution behavior of the spent fuel, in particular, the dissolution rate of the fuel matrix, the release rate of individual radionuclides, the form in which the radionuclides are released, and the mode of reaction.

Two irradiated PWR fuels, ATM-103 and ATM-106, are being tested in three types of unsaturated tests. The surrogate water, EJ-13, came from well J-13 and was equilibrated with volcanic tuff for approximately 80 days at 90°C. The seven tests have undergone 28 months of testing at 90°C as of the end of January.

Effort this month was devoted to three areas: (1) a new test plan was prepared and is being reviewed internally; (2) analysis of the ICP-MS data was begun; and (3) gamma results for the leachate and strip solutions for the drip tests sampled in October-November 1994 (~750 days of reaction) were analyzed.

The cesium gamma results for the leachate and strip solutions for the drip tests (~750 days of reaction) were compared to determine if the cesium remained in the leachate. The percentage of cesium sorbed on the test vessels appears to differ as a function of drip rate. For low drip rate tests, 99% of the cesium was sorbed on the stainless vessel walls; whereas for high drip rate tests, 99% of the cesium was in the leachate. Since the leachate of the four tests have comparable pHs (6.8-7.2), other factors appear to be responsible for this behavior.

1.2.2.4.2 Borosilicate Glass

D-20-27, Unsaturated Testing of WVDP and DWPF Glass

The N2 Unsaturated Tests on actinide- and technetium-doped SRL 165 glass have been ongoing for approximately 108 months. They were last sampled, as scheduled, on 12/19/94. In addition to the analyses required by the procedure, sequential filtering was performed on a portion of the solution, and colloid samples were extracted from the N2#10 test solution for analytical electron microscopy (AEM) analysis. Preliminary AEM results on these colloids indicate that they consist of clays and iron-silicates, some of which contain trace (~0.1-1 atomic %) uranium. Alpha spectroscopy of the sequential filtering samples will indicate if substantial transuranics are incorporated into the colloids.

The N3 Unsaturated Tests, performed on actinide-doped West Valley ATM-10 glass, were sampled on 1/12/95. They have been ongoing for 90 months, and are next scheduled for sampling on 7/13/95. Again, in addition to the analyses required by the procedure, sequential filtering was performed and colloidal samples for AEM analysis were taken from N3#9, #10, and #12. An apparent variation among the test samples regarding the corrosion of the stainless steel components is emerging; the N3#9 metal components appear the most reacted, while those of N3#10 are least reacted. Thus, interactions between waste package components will be important conduits for reaction and potential methods for mobilization of radionuclides.

1.2.2.5 Waste Package Materials Testing and Modeling

1.2.2.5.1 Metallic Barriers

The purpose of the metallic barrier task is to characterize the behavior and determine the corrosion rates and corrosion mechanisms of metallic barriers, including the interaction with the surrounding environment. Tests and modeling are performed to determine this behavior. Conceptual models of corrosion processes are developed for use in evaluating waste package performance. This task provides considerable input on materials properties to the waste package and repository design tasks and to the performance assessment task.

Degradation Mode Surveys (PACS OL251LGI)

A procurement package for the conduct of a "Degradation Mode Survey" on Monel 400 class Ni-Cu alloys is being rewritten to satisfy the stringent criteria for a "sole source procurement" that has been set forth by LLNL Procurement. G. Gdowski is preparing a draft of a "Degradation Modes Survey" for titanium alloys.

Performance Tests and Model Development (PACS OL251LGK)

G. Henshall's work focused on the new capability of the "PIGS" stochastic model to simulate the permanent cessation of growth for "stable" (i.e., macroscopic) pits. As described in the December, 1994 report, the existing PIGS code was modified to include a new stochastic variable, η , describing the probability that stable pits permanently halt their growth. Further, that report discussed two possible ways to view pit growth with cessation: (1) pit growth is fundamentally stochastic and includes the possibility that pits may permanently stop growing; and (2) pit growth is fundamentally deterministic and continuous, but individual pits may stop growing at different times during exposure. The focus of efforts this month was on the first possibility, which can be explored using $0 < \eta < 1$ and a pit growth probability, γ , less than one.

The investigation of how permanent pit growth cessation affects the damage function (i.e., the distribution of pit depths) continued by extending the calculations began last month. In these numerical experiments, a 635-cell model was used with a stochastic pit growth probability of $\gamma = 0.05$ and various values of the pit growth cessation probability, $\eta = 0.05, 0.01, 0.005$ and 0.001 . The results of these simulations are given in Figures 1-4. For the relatively large value of $\eta = 0.05 = \gamma$, the distribution maintains an "exponential decay" type of shape for all exposure times. An example of this distribution is shown in Figure 1 for exposures of 200 steps or greater, for which the distribution is "static", i.e., all pits have stopped growing. For a value of $\eta = 0.01 = \gamma/5$, the distribution has two local peaks for all but the shortest exposure (40 steps). The first peak always occurs at the lowest pit depth. As exposure time increases, the second peak decreases in height and a "tail" is developed at the larger depths. By 500 steps, the distribution becomes essentially static with the shape shown in Fig. 2. Although the small second local peak is still apparent at a depth of 3 (arbitrary units), the overall distribution has the exponential decay shape. Decreasing the halt probability further to $\eta = 0.005 = \gamma/10$ leads to a complex evolution of the distribution from one similar to that shown in Figure 1, through single-peak and "plateau" shaped distributions. Ultimately, at an exposure of 1000 time steps, the distribution becomes static with an exponential decay type of the shape shown in Figure 3. This decay occurs over a much wider range in pit depths than the static distributions for larger values of η , Figures 1 and 2. Finally, for $\eta = 0.001 = \gamma/50$ the distribution evolves from one similar to that shown in Figure 1, through single and double-peak distributions (similar to those for $\eta = 0.01$) toward a very gently decaying distribution spread over a very wide range of pit depths. A nearly static distribution is reached following 4000 steps of exposure. Figure 4 shows that this distribution exhibits a gradual exponential-type decay in the number of pits vs. their depth, although there is a large variability from one pit depth to the next.

The previous discussion suggests that, in general, the effect of pit growth cessation is the ultimate development of a static distribution with essentially an exponential-like decay in the number of pits as a function of depth. As the halt probability, η , decreases, the rate of this decay decreases and the distribution broadens. As described in previous reports (Jan. 1994, Nov. 1994), the experimental data suggest that the pit depth distribution following long exposure times is more complex than this; typically, it contains a significant intermediate peak. Of course, it is necessary to explore a wider combination of γ (and other input) values to confirm the generality of these observations. Next month, calculations will continue using the "deterministic pit growth" option of $\gamma = 1$ (with $0 < \eta < 1$). Again, the major goal will be to determine if distributions similar to those observed experimentally can be simulated using this approach.

Figure 1.

Pit damage function for 5% growth probability and 5% cessation probability

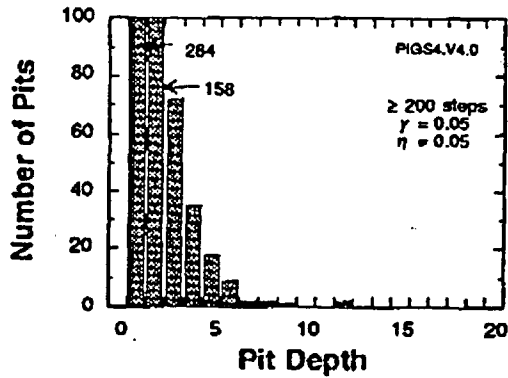


Figure 2.

Pit damage function for 5% growth probability and 1% cessation probability

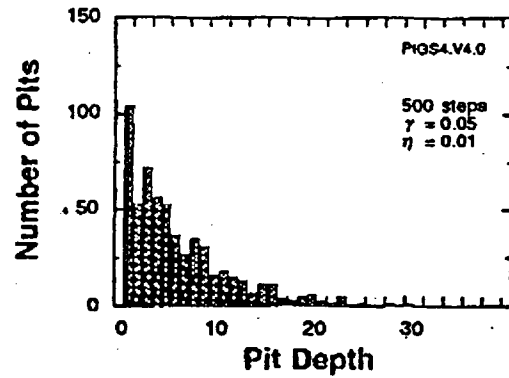


Figure 3.

Pit damage function for 5% growth probability and 0.5% cessation probability

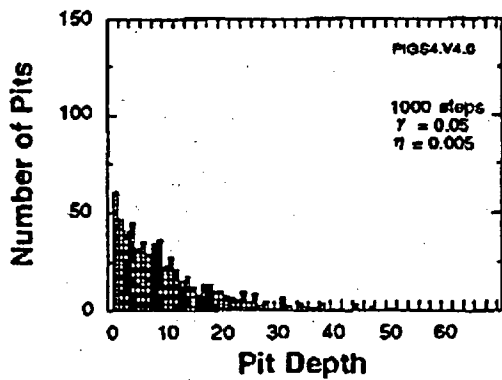
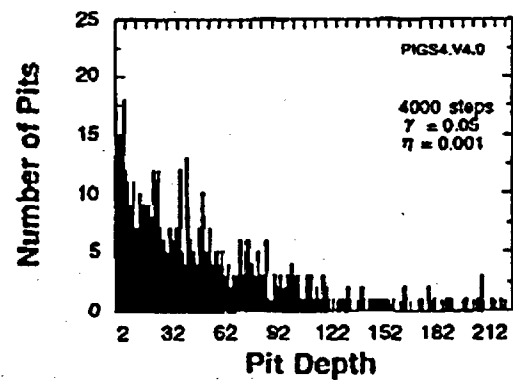


Figure 4.

Pit damage function for 5% growth probability and 0.1% cessation probability



Thermogravimetric Analysis

J. Estill and S. Gordon are working on two issues with the TGA. The software supplied by Cahn, Inc. continues to "crash" during the course of a test. The manufacturer has supplied a laptop PC for process monitoring to capture the crash as it occurs. Two tests in which the error occurred have been captured and stored on the laptop hard drive. The laptop was returned with the captured data, and we expect to hear from the manufacturer in the next few days.

The problems associated with noise generation during the conduct of a typical TGA test are persisting. Spikes in temperature and humidity are noted when water vapor is introduced into the reaction tube. LLNL staff met with an experimenter who has some experience with the Cahn microbalance, and he provided a list of possible problems when testing in a water vapor environment. Unfortunately, his experience was limited to very low concentrations of water vapor (~1 ppm), which is much less than concentrations of water present in a saturated environment. Some of the suggestions given by the experimenter will be implemented in the next few months.

Long Term Corrosion

G. Gdowski reviewed the literature to determine acceptable weld processes for welded specimens for the long-term corrosion tests. A table of weld processes parameters was prepared by G. Gdowski and J. Estill and reviewed by E. Dalder. These weld processes will be used for the test specimens and are contained in the Comprehensive Specimen Configuration (CSC).

J. Estill has completed the CSC, including a listing of 50,000 specimens (with referenced drawings) of C-rings, crevice, weight loss, and galvanic coupons, and the table of weld processes, for the seven candidate alloys. The CSC was reviewed in detail, and comments were incorporated. The CSC has been submitted to a metal sample supplier for pricing information. Design of individual corrosion test vessels will proceed as soon as the final CSC is established, which should be within the next month.

R. Green completed a system document, "Specifications/Requirements for Process Monitor and Control and Safety Interlocks", which describes the control and data acquisition system requirements for the long term corrosion tests. The document was reviewed.

J. Estill and R. D. McCright submitted a UCID report for publication entitled "Corrosion of Candidate Materials in Lake Rotokawa Geothermal Exposure". The draft is currently in technical review. The report describes the corrosion rate calculations for and qualitative observations of the corrosion product and surfaces of flat coupons, crevice plates, and U-bends after six weeks exposure in a 90°C pH 2 geothermal spring in New Zealand. Metallographic cross sections of typical samples are included. Alloys CDA 613, CDA 715, CDA 102, Incoloy 825, ASTM A 36 and 1020 carbon steel, and type 304L austenitic stainless were tested in this environment.

A purchase order for several high performance alloys has been prepared. These samples are for follow-up tests in environments similar to those in the Lake Rotokawa, NZ area.

Crack Growth Tests (PACS OL251LGO)

The purpose of this work is to determine the stress corrosion cracking (SCC) susceptibility of candidate waste container materials under a variety of environmental, metallurgical, and

mechanical stress conditions relevant to a repository. Stress corrosion is an important degradation mode that can affect both corrosion-allowance and corrosion-resistant materials. A sensitive crack growth measurement apparatus, which operates under the principle of measuring minute changes in the electrical resistance of the test specimen as a crack propagates, is in use at Argonne National Laboratory (ANL) to measure crack growth on pre-cracked compact tension fracture mechanics type of specimens. A similar unit is being commissioned at LLNL. Research activities deal with fracture mechanics crack-growth-rate determinations on Incoloy 825, Titanium Grade 12, Hastelloy C-4, and Hastelloy C-22. Crack growth rate (CGR) tests using standard compact tension (CT) fracture mechanics specimens have been conducted on Incoloy 825 in an earlier phase of the program. Additional tests were initiated on Ti Grade 12, Hastelloy C-4, Hastelloy C-22, and on a new heat of Incoloy 825 in FY94.

Crack growth rate tests are continuing for standard Titanium Grade 12 (Specimen No. T16-01), Hastelloy C-22 (Specimen No. 227-01) and Hastelloy C-4 (Specimen No. 245-02) in a simulated J-13 well water environment at 93°C. The simulated J-13 well water was prepared from deionized high-purity water and reagent-grade-purity salts of CaSO₄, Ca(NO₃)₂, CaCl₂, FeCl₂, Li₂SO₄, MgSO₄, MnSO₄, AlCl₃, Na₂CO₃, NaHCO₃, KHCO₃, Na₂AlO₃, and HF. High-purity mixed gas containing 20% O₂, 12% CO₂, and 68% N₂ is used as a cover gas at 20-34 kPa (3-5 psig) to maintain the desired dissolved O₂ and HCO₃ concentrations. The pH value of the feed water is in a range of 6-8. The specimens have been fatigue-cracked in air at room temperature for a precrack length of 1.9 mm under a cyclic load with triangular load shape, load ratio of R = 0.1 to 0.25 and loading-frequency of 1 Hz, to introduce a sharp-starter crack before crack-growth rate-tests.

Preliminary data show that the crack propagates faster in the Titanium Grade 12 specimen than in the Hastelloy specimens by an order of magnitude, under a 0.5 Hz cyclic load with triangular load shape, load ratio of R = 0.5 and stress intensity range of $26 \pm 28 \text{ MPa}\cdot\text{m}^{1/2}$ in J-13 well water. Growth rates of 1.1×10^{-8} , 0.90×10^{-8} , and 1.1×10^{-8} m/s were observed for the Titanium Grade 12 (Specimen No. T16-01), Hastelloy C-22 (Specimen No. 227-01) and Hastelloy C-4 (Specimen No. 24 5-02), respectively.

Microbiologically Influenced Corrosion

A preliminary proposal was obtained from Professors D. Jones (UNR) and P. Amy (UNLV). Topics to be worked on include:

- 1) Electrochemical Detection of MIC - Develop test procedures to determine MIC susceptibility of steel in water samples taken during exploratory and construction phases of repository operations.
- 2) Electrochemical Stimulation of Corrosion by Bacterial Growth - Determine electrochemical interactions between corrosion and bacterial growth, including cause and mechanism of localized MIC at weldments.
- 3) Effects of Elevated Temperature and Nutrient Availability on Bacterial Growth and Subsequent MIC - Study the ability of microbial cultures from Rainier Mesa and Yucca Mountain to revive, grow and cause corrosion at elevated temperature.

The first two topics would be conducted by Prof. Jones at UNR, and the third topic would be conducted by Prof. Amy at UNLV. Negotiations on budgetary and schedule matters have begun.

1.2.2.5.2 Basket

The objective of the Basket Materials task is to assemble property data on candidate materials for use in the support baskets for spent fuel in waste containers and to aid in the selection of materials for this purpose. The baskets must provide mechanical support, must assist in heat transfer, and must absorb neutrons to provide long-term criticality control.

On January 18, R. Van Konynenburg and R. D. McCright met with D. Stahl and T. Doering of B&W Fuels Co. to discuss milestones and interfaces between the waste package design effort and the waste package materials evaluation effort. Because work on basket materials represents a new effort, these interfaces are particularly vital in the initial activities. The next milestone is March 15 when the Scientific Investigation Plan is due. On August 31, a report on scoping tests is due.

Possible candidate basket materials, including metals and ceramics were discussed. T. Doering agreed to look into the criticality control properties of Zr-Hf alloy with Hf present in amounts found naturally in Zr ores, and he supplied a copy of earlier control rod and control panel studies.

R. Van Konynenburg had prepared and submitted to A. Segrest (Duke Engineering) an 11 page draft entitled "Corrosion Considerations in Choosing MPC Basket Materials" which was discussed. On January 27, R. Van Konynenburg discussed this draft by phone with H. Cleary of Weston, Inc., who has been asked by J. Williams of DOE to review the issue of MPC basket material selection. The draft report was faxed to H. Cleary.

1.2.3 SITE INVESTIGATIONS

1.2.3.1 Site Investigations Coordination and Planning

Groundwater Travel Time (GWTT) Distribution and Repository Performance

The GWTT standard was intended to be a simple measure of the geologic quality of a repository site, independent of total system performance. Unfortunately, it is neither independent nor simple. The GWTT standard is not independent because the travel time reflects the distribution of groundwater flux among all pathways connecting the repository to the accessible environment (AE). Since liquid water is believed to be the principal medium for the transport of radionuclides, the radionuclide flux entering the AE will be directly related to the amount and spatial distribution of water flowing from the repository to the AE, and to the sorption coefficients and solubilities of the radionuclide species released from the engineered barrier system (EBS).

The GWTT standard is not simple because there is no single number for the GWTT: it must be represented by a distribution, as acknowledged in the 1985 letter to the DOE from the Director of the NRC Division of Waste Management. However, *the GWTT distribution does not arise from uncertainty* in our understanding of the geologic system. The following points describe the GWTT:

- GWTT in any real system typically ranges over two or more orders of magnitude.
- In principle, the GWTT distribution is a deterministic function of the spatial distribution of hydrologic properties (permeability, porosity, saturation, ...), the flow system geometry, and the boundary and initial conditions of the system.
- Conceptually, the distribution could be experimentally determined by releasing a non-sorbing tracer at a known rate for a known time at the repository horizon and measuring the total tracer mass reaching the AE as a function of time. This is the *breakthrough curve*.

- The spatial and temporal scale of the repository precludes actually conducting such an experiment, but cosmogenic radioisotopes provide a natural tracer test, and particle-tracking model calculations attempt to simulate one.
- The distribution of GWTT is governed by the heterogeneity of flow velocities, which is usually dominated by the spatial variation of permeability and flow path geometry.
- No amount of characterization data will reduce the spread of GWTT arising from heterogeneity.
- Uncertainty in the model parameters introduces a distribution of distribution functions.

The GWTT issue can be stated as follows:

1. In a heterogeneous system, a non-zero fraction of the total groundwater flow, $F(1000)$, will have a travel time less than or equal to 1000 years.
2. At Yucca Mountain, observations of bomb-pulse tritium in the Calico Hills, along with ^{36}Cl bomb-pulse data, strongly suggest that an unknown fraction of water infiltrating from the surface reaches the water table in a few decades.
3. Although water reaching the water table still must travel about 5 km to reach the AE, it is difficult to argue convincingly that *no* water will reach the AE in less than 1000 years under pre-emplacement conditions.
4. Given that $F(1000) > 0$, how large can the "fast fraction" be and still allow reasonable assurance of meeting total system performance requirements?

The use of total system performance analysis (TSPA) to evaluate the significance of travel times less than 1000 years seems to be the only reasonable way to address this question. However, NRC staff are concerned that using TSPA to determine the significance of "fast pathways" with values of travel time less than 1000 years destroys the intended function of GWTT to provide an independent measure of the ability of the site to isolate radionuclides from the accessible environment. TSPA calculations include detailed models for the failure of the Waste Packages (WPs) and consequent release of radionuclides from the EBS to the geosphere, and there is no simple way to separate the contributions of the EBS and the hydrogeologic system in controlling the release of radionuclides to the AE.

The EBS and geosphere contributions can be assessed separately with the aid of a simple analytic model for bounding the release of radionuclides to the accessible environment (Dwayne A. Chesnut, "Groundwater Flux, Travel Time, and Radionuclide Transport," UCRL-JC-116436, October 1994).

The significance of "fast pathways" can be assessed by *assuming* exact compliance with the EBS subsystem requirements (substantially complete containment and controlled release) and calculating the release to the AE for combinations of various log-normal distributions of GWTT, and using parameters for a reference radionuclide inventory.

The problem of *demonstrating* EBS subsystem compliance still remains, but *assuming* subsystem compliance allows evaluation of what is required from the groundwater transport system to meet the total system release standard without considering any details of the EBS performance. The important point here is that no special emphasis is placed on the EBS: it only meets the minimum requirements.

Total system release to the AE was calculated by evaluating the convolution integral for each of 29 radionuclides to obtain its release rate as a function of time, integrating the AE release rate over 10,000 years, normalizing the result by the applicable EPA limit, and then summing over the

radionuclides. By requiring the sum to equal 1.0 and 10.0, respectively, the upper and lower curves in Fig. 5 were calculated. These show combinations of GWTT distribution parameters required to give these two fixed values of the EPA sum. Above the upper curve, the EPA sum is less than 1; regulations require reasonable assurance that the probability is 0.9 or greater that this sum will be met. Compliance also requires reasonable assurance that the probability is at least 0.999 that parameters will lie in the region above the lower curve. For $\sigma = 0$ (a completely homogeneous system), a GWTT of 1057 years is sufficient to assure compliance with the total system performance requirement. As the system becomes increasingly heterogeneous (*i.e.*, σ increases), a longer mean GWTT is required.

A heterogeneity parameter of $\sigma = 1.6$ fits the inflow flux distribution at Stripa measured by Abelin and others, and a value of about 2.2 fits the distribution of hydraulic conductivity obtained from pump tests of the Calico Hills in the saturated zone, tabulated by Loeven. A mean GWTT of about 70,000 years is required to make the EPA sum equal to 1.0 when the heterogeneity parameter is equal to 2.2. Since transport through the unsaturated zone at Yucca Mountain is through the Calico Hills, this degree of heterogeneity should be used in performance calculations until other data become available.

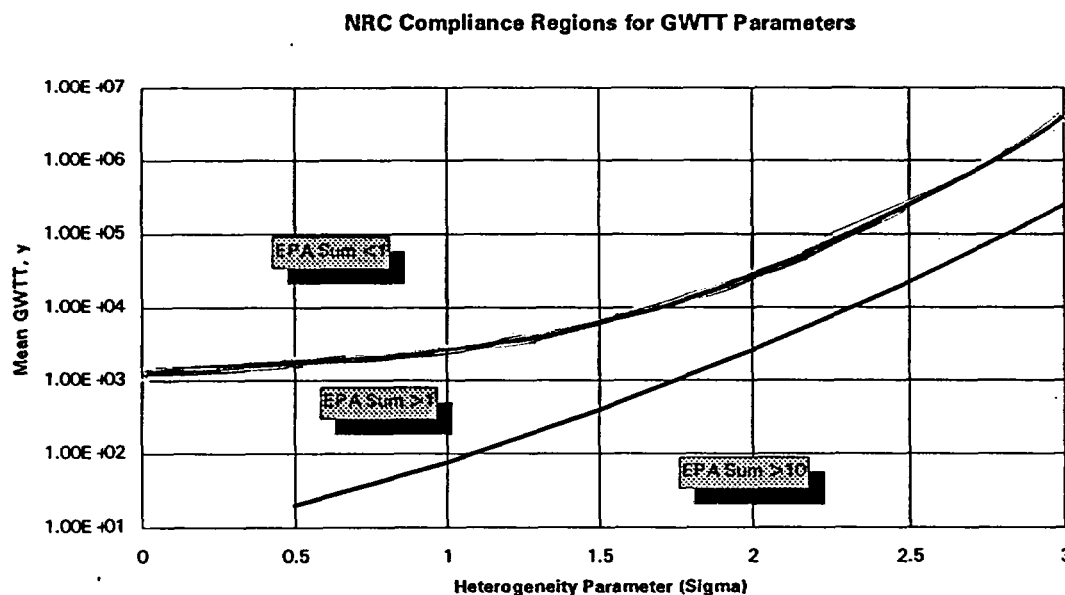


Figure 5. Groundwater travel time distribution parameters corresponding to compliance and non-compliance with total system release standards. Along the upper curve, the EPA sum is equal to 1.0, and along the lower curve, it is equal to 10.0

The mean GWTT corresponds to a hypothetical system having the same total liquid throughput rate and the same liquid-filled pore volume as the real system, but with uniform linear flow from the inlet to the outlet. By neglecting the travel time after groundwater reaches the water table, we can get a conservative estimate for mean GWTT to use in transport calculations. For liquid filled fractional porosity on the order of 0.10, and an average distance from the repository horizon to the water table on the order of 250 meters, the mean GWTT is $(25,000/I_w)$ years where I_w is the infiltration rate in mm/year. If the infiltration rate is 0.1 mm/year, as often assumed, the mean travel time is 250,000 years, and there would be no difficulty showing, in the context of this

bounding calculation, that the total release standard would be met for σ up to about 2.5. On the other hand, if I_w is 1 mm/year, then the system must be much more homogeneous to meet the GWTT standard, with a σ less than about 1.8. Finally, if I_w is 10 mm/year (a value which cannot be excluded based on available data), the mean GWTT would be only 2,500 years, and σ must be less than about 0.8 for GWTT compliance. A value much less than 1.5 seems very unlikely if fractures contribute to the flow and transport in the unsaturated zone below the repository.

We can now consider the question asked above: How large can the "fast fraction" be and still allow reasonable assurance of meeting total system performance requirements? Fig. 6 is a plot of the fraction of groundwater having a travel time less than 1,000 years for the GWTT parameter combinations of t_w and σ that result in a value of the EPA sum of 1.0 (from the upper curve in Fig.5).

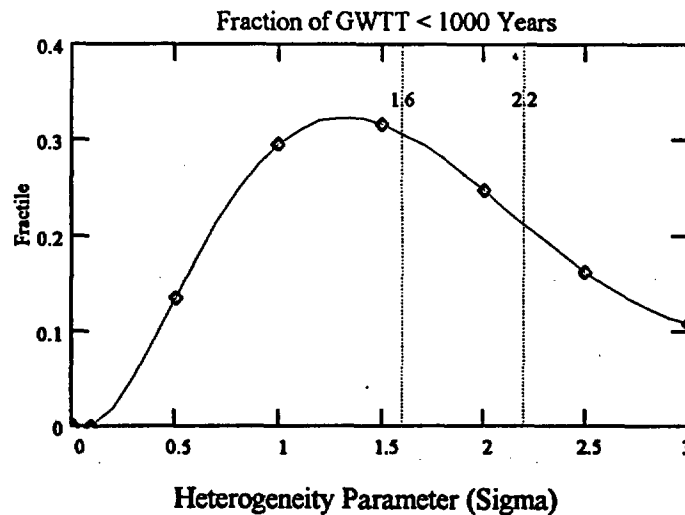


Figure 6. The fraction of groundwater flow with a travel time less than or equal to 1,000 years for combinations of mean GWTT and heterogeneity that produce the upper curve in Fig. 5.

This plot shows that up to about 30% of the groundwater could have a travel time of less than 1000 years from the repository to the accessible environment and still permit a demonstration of compliance with the total system release standards. The maximum in this plot indicates that the greatest tolerance to "fast paths" would be obtained for a σ of about 1.3.

These calculations suggest that, *in a strongly heterogeneous system with a large mean travel time*, a rather large fraction of the total groundwater flux could have a travel time much less than 1,000 years and still allow satisfactory containment of radionuclides within the geologic control volume.

The observation of bomb-pulse isotopes over most of the depth of the unsaturated zone must be accommodated in any satisfactory analysis of site-scale transport. These observations indicate some transport from the surface essentially to the water table in 40 years or less. What are the total system performance implications of this rapid transport?

Figure 7 shows the fraction of infiltrating water having a travel time less than 40 years for the same combinations of GWTT parameters used in Fig 6. For a heterogeneity parameter greater

than about 2, more than 1% of the total groundwater infiltration would have a travel time of less than 40 years. For a heterogeneity parameter less than 1, a negligible fraction would have a travel time less than 40 years. In other words, the system must be somewhat heterogeneous to simultaneously account for the observed frequency of occurrence of bomb-pulse material at depth and to demonstrate total system compliance if the system is too homogeneous.

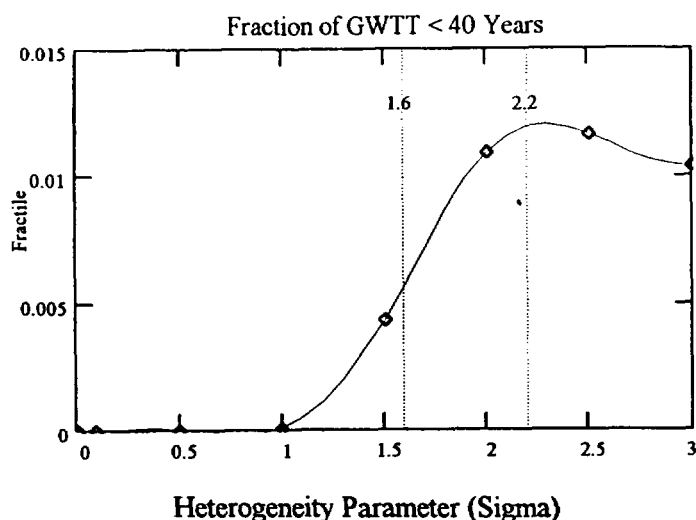


Figure 7. The fraction of groundwater flow with a travel time less than or equal to 40 years for combinations of GWTT parameters used in Fig. 6.

Since bomb pulse isotopes have been observed at depth, these calculations suggest that σ is likely to be closer to 2 than to 1, or, alternatively, that the mean GWTT is much shorter than the value required to bound the total system release within the regulatory requirement.

This analysis does not imply that these are the "correct" values of GWTT parameters to use in performance calculations for Yucca Mountain, since the actual combination of values would almost certainly not lie on the EPA compliance curve used in the calculations.

LLNL is developing an approach, in collaboration with Fabryka-Martin of LANL and others, for using the bomb pulse data quantitatively to estimate parameters for the log-normal distribution of GWTT. Although the analyses are not complete due to the limited number of data points available, it appears that relatively large values of both the heterogeneity parameter and mean GWTT will be needed to obtain consistency with the observed frequency of occurrence of bomb-pulse isotopes throughout Yucca Mountain.

1.2.3.11 Integrated Geophysical Testing for Site Characterization

1.2.3.11.2 Surface-Based Geophysical Testing

LLNL performed logging operations at USW-SD7 on January 5 and 31 and at USW G-2 January 3. Photo inspections of the drill holes were conducted. On January 3, a logging operation was conducted at USW G-2 in order to obtain a fluid sample.

LLNL assisted Slumberger Logging Co., as directed by SAIC, on January 3-11. Attempts to run the gravimeter in UE25-UZ16 were unsuccessful. The gravimeter is being returned to the manufacturer in Austin, Texas for repair.

1.2.3.11.3 Geophysics—ESF Support, Subsurface Geophysical Testing

LLNL performed construction logging in Alcove #1 of the Exploratory Studies Facility (ESF) on January 24-26, 1995. The logging consisted of borehole caliper and borehole color camera runs in the horizontal boreholes RBT #1, RBT #2, and RBT #3. Data were successfully recovered from all the logging runs and valuable experience was obtained which will help us finalize the Technical Implementation Procedure for Underground Logging.

1.2.3.12 Waste Package Environment Testing and Modeling

1.2.3.12.3 Mechanical Attributes of the Waste Package Environment

The objective of this task is to characterize the geomechanical response of the rock in the near-field to the changing conditions expected to occur over the lifetime of the repository. This includes providing data from laboratory, field and modeling investigations that can be used to support technical site suitability and a high level finding for rock properties. Particular emphasis is on coupled processes and behavior at elevated temperatures and at long times. Work conducted on this task during January is listed below.

Laboratory

A second suite of uniaxial compression tests was conducted on a sample block of Topopah Spring Tuff that measures 64 x 33 x 25 cm (25 x 13 x 10 inches) in size. Analysis of the stress-strain behavior indicates a similar modulus to that reported in December (modulus = 3 GPa for axial stress in the range 0-5 MPa) and that, as expected, most of the deformation occurs across fractures. In addition, noticeable spalling occurred at several locations on the block. This was not observed during the first cycle of testing and indicates that subcritical crack growth occurs even at very low stresses in this rock when it is subject to cyclic loading. This may be relevant for evaluating the effect of seismic shaking of the potential repository over long times and at elevated temperature and humidity.

Compressional wave velocity was also measured in a few blocks of Topopah Spring Tuff from the Fran Ridge site at ambient temperature and pressure conditions. Preliminary results show the P wave velocities to be in the range 3.8 to 4.7 km/s, in agreement with result from the G-Tunnel tests. In addition, elastic waves traveling through unfractured tuff were about 10% faster than waves that had significant parts of the travel path passing through fractured rock.

In addition, scanning electron microscope (SEM) backscatter images were produced at a variety of magnifications for sections of core samples from hole NRG-6. These are samples that showed significant thermal expansion with increasing temperature, attributed to the phase transition of cristobalite or other mineral phases. Sections were also examined that were prepared from unheated sample material. No significant differences in microstructure were apparent upon preliminary examination between the heated and unheated samples, and more detailed analysis is underway.

Modeling

An agreement was reached with H. Wang (U. Wisconsin) to consult on the geomechanics modeling task. Herb is an accomplished researcher and will provide advice on the applicability of selected geomechanics codes to the YMP, evaluate thermal stresses in the region near the heaters in the field tests, and assess the importance of thermoelastic and poroelastic behavior in the near-field over the lifetime of the repository.

LLNL PROJECT STATUS REPORT EXTERNAL DISTRIBUTION

January 1995

W. Barnes
YMSCO
Department of Energy
101 Convention Center Dr.
Las Vegas, Nevada 89109

Dr. J. Bates
Chemical Technology
Argonne National Laboratory
9700 S. Cass Avenue
Argonne, Illinois 60439

H. Benton
M&O, M/S 423
101 Convention Center Drive
Las Vegas, NV 89109

A. Berusch (RW-20)
OCRWM
Forrestal Building
Washington, DC 20585

J. Blink
LLNL/Las Vegas
101 Convention Center Drive, Suite 880
Las Vegas, NV 89109

B. Bodvarsson
LBL/Earth Sciences
Bldg. 50 E
1 Cyclotron Road
Berkeley, CA 94720

S. Brocoum
YMSCO
101 Convention Center Dr.
Las Vegas, NV 89109

J. Canepa
Los Alamos National Laboratory
P.O. Box 1663/N-5, MS J521
Los Alamos, NM 87545

P. Cloke
Science Applications Int'l Corp.
101 Convention Center Dr., #407
Las Vegas, NV 89109-2005

C. Conner
DOE, RW-133
1000 Independence Ave., SW
Washington, DC 20585

R. Craun
YMSCO
P.O. Box 98518
Las Vegas, NV 89193-8518

C. DiBella
NWTRB
1100 Wilson Blvd., Suite 910
Arlington, VA 22209

T. Doering
M&O
101 Convention Center Dr., MS 423
Las Vegas, NV 89109

D. Dresser
Roy F. Weston, Inc.
955 L'Enfant Plaza, SW
8th Floor
Washington, DC 20024

J. Dyer
YMSCO
Department of Energy
P.O. Box 98518
Las Vegas, NV 89193-8518

R. Einziger
Battelle-Pacific Northwest
P.O. Box 999/MS P714
Richland, WA 99352

J. Farrell
M&O TRW
TES1/3573
Vienna, VA 22180

R. Fish
M&O
101 Convention Center Dr., M/S 423
Las Vegas, NV 89109

A. Gil
YMSCO
Department of Energy
P.O. Box 98518
Las Vegas, NV 89193-8518

R. Green
Southwest Research Institute
6220 Culebra Rd.
San Antonio, TX 78238-5166

L. Hayes
U.S. Geological Survey
Box 25046/MS 425
Denver Federal Center
Denver, CO 80225

R. Hughey
Nuclear Energy Division
US DOE/OAK
1301 Clay St., Rm. 700-N
Oakland, CA 94612

C. Johnson
M&O
101 Convention Center Dr., M/S 423
Las Vegas, NV 89109

N. Jones
M&O
101 Convention Ctr. Dr., M/S 423
Las Vegas, Nevada 89109

S. Jones
YMSCO
Department of Energy
101 Convention Center Dr.
Las Vegas, NV 89109

H. Kalia
Los Alamos National Laboratory
101 Convention Center Dr., Suite 820
Las Vegas, NV 89109

S. Kennedy
OCRWM
Forrestal Bldg.
Wash., D.C. 20585

S. Marschman, P7-14
Battelle, Pacific Northwest
P.O. Box 999
Richland, WA 99352

S. Nelson
M&O
101 Convention Center Dr., M/S 423
Las Vegas, NV 89109

R. Robertson
TRW-Metro Place
2650 Park Tower Dr., Suite 800
Vienna, VA 22180

D. Rogers
M&O
101 Convention Center Dr., M/S 423
Las Vegas, NV 89109

S. Saterlie
M&O LV
101 Convention Center Dr., M/S 423
Las Vegas, Nevada 89109

D. Schutt
M&O LV
101 Convention Center Dr., M/S 423
Las Vegas, Nevada 89109

A. Segrest
M&O
101 Convention Center Dr., M/S 423
Las Vegas, Nevada 89109

L. Shepherd
Sandia National Laboratories
M/S 1333
P.O. Box 5800
Albuquerque, NM 87185-1333

A. Simmons
YMSCO
Department of Energy
P.O. Box 98518
Las Vegas, Nevada 89193-8518

E. Smistad
YMSCO
Department of Energy
P.O. Box 98518
Las Vegas, Nevada 89193-8518

M. Smith
YMSCO
Department of Energy
P.O. Box 98518
Las Vegas, Nevada 89193-8518

L. Snow
Roy F. Weston, Inc.
955 L'Enfant Plaza, SW
Washington, DC 20024

H. Spieker
M&O
101 Convention Ctr Dr., M/S 423
Las Vegas, NV 89109-2005

D. Stahl
M&O/B&W
101 Convention Ctr. Drive, M/S 423
Las Vegas, NV 89109

D. Stucker
YMSCO
Department of Energy
P.O. Box 98518
Las Vegas, Nevada 89193-8518

A. Van Luik
M&O
101 Convention Ctr. Dr., M/S 423
Las Vegas, NV 89109

G. Vawter
M&O/TRW
101 Convention Center Dr.
Las Vegas, NV 89109

M. Voegele
M&O/SAIC
101 Convention Center Dr., #407
Las Vegas, NV 89109-2005

M. Weaver
M&O
101 Convention Center Drive, M/S 423
Las Vegas, Nevada 89109

N. White (3)
Nuclear Regulatory Commission
301 E. Stewart Ave. #203
Las Vegas, NV 89101

D. Williams
YMSCO
Department of Energy
P.O. Box 98518
Las Vegas, Nevada 89193-8518

J. Younker
M&O/TRW
101 Convention Center Dr.
Las Vegas, NV 89109

P. Zielinski
YMSCO
Department of Energy
P.O. Box 98518
Las Vegas, Nevada 89193-8518